Global-scale Multidecadal Climate Variability: The Stadium Wave

Sergey Kravtsov[1,2], Andrew Westgate[3], and Andrei Gavrilov[4]

[1]University of Wisconsin-Milwaukee, [2]Shirshov Institute of Oceanology RAS,
[3]Vermont State University, [4]Image Processing Laboratory, University of Valencia

Session: NP3.3 - Extreme variability across scales, from theory to applications; Presentation number: EGU26-7074;
Display time: Friday, 8 May 2026, 8:30-12:30 (author in attendance time: 10:45–12:30); Location: Hall X, board X4.4

Introduction

Twentieth-century climate variations exhibit, on top of the secular global warming trend, multidecadal variability with globally coherent patterns (Deser and Phillips 2017). The amplitude of this variability is outside of the envelope of global climate model simulations (Kravtsov et al. 2018; Wills et al. 2022). We here apply a suite of pattern-recognition methods to succinctly characterize such variability in a 38-model CMIP5/6 ensemble of historical simulations and two reanalysis data sets: Twentieth Century Reanalysis (20CRv3: Slivinki et al. 2019) and ECMWF Reanalysis of the Twentieth Century (ERA-20C: Poli et al. 2016) and test the hypothesis that the spatiotemporal structure of the observed multidecadal variability can be explained by that of the inter-model forced-signal uncertainty.

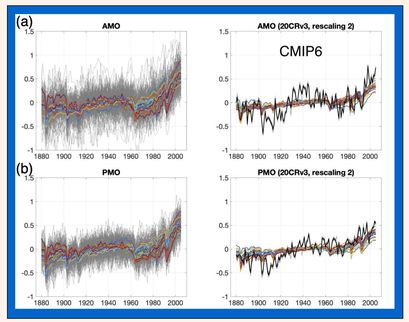

Fig. 1: Unscaled (left) and rescaled (right) forced signals of individual models (colored curves) on top of the grand ensemble of the historical simulations (left, gray curves) or reanalysis time series (right, black curves) for two SST climate indices: AMO and PMO.

Forced-signal estimation

Following Wills et al. (2020), we use signal-to-noise maximizing S/NP filtering on top of ensemble averaging of individual-model simulations to estimate 38 forced signals in gridded near-surface air temperature (SAT) over the global domain in all the models considered (Fig. 1, left, shows forced response in AMO and PMO climate indices). We also apply a new pattern-based rescaling to best fit the individual forced signals to observations, which reduces the raw spread of these signals (Fig. 1, right). These rescaled signals are used in lieu of the observed forced signals. Finally, we use the S/NP analysis to identify the common evolution (**Fig. 2**) and individual residuals in the 38-member forced-signal ensemble (see below).

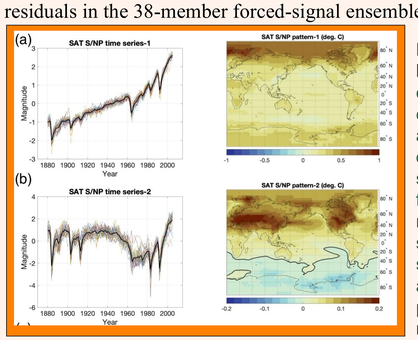

Fig. 2: The two leading S/NP modes characterizing the common evolution across the ensemble of 38 SAT forced-signal estimates from individual models, with time series (components) shown on the left, and dimensional patterns — on the right.

Forced-signal decomposition

The two leading S/NP modes that dominate the common evolution among the 38-member forced-signal ensemble (Fig. 2) are associated, for mode-1, with a polar-intensified global warming response which exhibited a substantial acceleration after 1980. By contrast, S/NP-2 is a land-intensified mode also associated with inter-hemispheric SAT contrast and multidecadal undulations. The trailing common S/NP modes are less ubiquitous and are generally associated with smaller contributions to the individual forced signals (Fig. 3a).

We found an interesting connection between the relative magnitudes of the S/NP modes 1 and 2 and a global-mean warming rate of individual-model forced signals (Figs. 3b–c). In particular, the models with high contributions from S/NP-1 and low contributions from S/NP-2 tend to exhibit faster warming rates and vice versa.

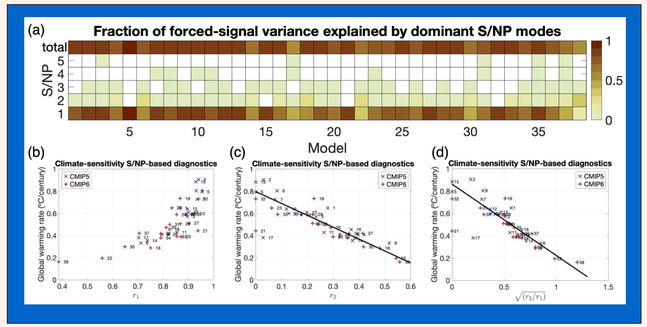

Fig. 3: (a) Fraction of variance r^2_k explained by the 38-forced-signal ensemble's common S/NP modes 1–5 (and their sum) in the individual forced signals. (b–c) Dependence of the global-mean temperature 1880–2005 linear-trend slope on the parameters r_1 and r_2: the models with large r_1 and small r_2 tend to exhibit larger trends.

Analysis of observed and forced-signal residuals

The main portion of our analysis deals with the identification of the dominant multidecadal variability in the residuals obtained by: (1) subtracting the model-estimated forced signals from the observed climate evolution, as well as (2) the 38 forced-signal residuals left after isolating the common evolution across the entire forced-signal ensemble. While the magnitude of the latter residuals (essentially, the forced-signal uncertainty) is much smaller than that of the observed residuals (see, for example, left panels of Fig. 1 here), it could still be possible that their spatiotemporal structure could mimic that of observations, lending support to the forced-signal origin of the observed multidecadal signal.

To document this structure, we first applied, to each gridded residual time series considered, a Multi-channel Singular-Spectrum analysis (M-SSA: Ghil et al. 2002) filter to isolate the reconstructed components of the leading M-SSA pair (Kravtsov et al. 2018). We then computed two leading rotated EOFs of the SAT data so smoothed in a way that the leading rotated EOF (AMO-like) pattern would be associated with the rotated PC maximally correlated with the AMO index, while the next EOF's (AMO-orth pattern) rotated PC would lag the first one. The observed signal (**Fig. 4**) was dubbed the **stadium wave** (Wyatt et al. 2012) and turns out be largely insensitive to methodological details. The analysis of forced-signal residuals (**Fig. 5**) identifies a mode of delayed forced response with a common pattern, but model-dependent time delay. In principle, this signal could explain some of the observed stadium wave, but its pattern correlations with observations are small (**Fig. 6**).

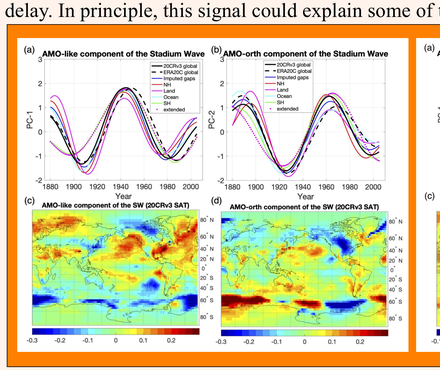

Fig. 4 : Time series (top) and (20CRv3) patterns (bottom) of the AMO-like and AMO-orth components of the global stadium wave (see text). The different curves in the top panel correspond to the estimates based on the alternative reanalysis data set or regional (or extrapolated) versions of the 20CRv3 analysis. They demonstrate the robustness of the observed stadium-wave signal.

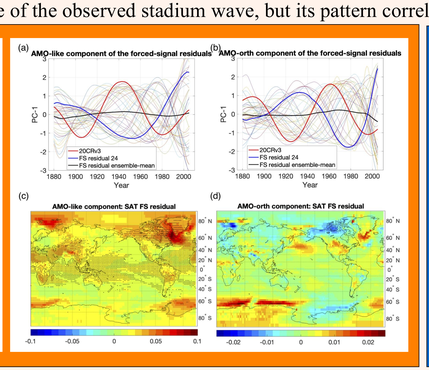

Fig. 5: An analog of Fig. 4, but for the analysis based on the 38 forced-signal residuals of the CMIP5/6 models. The (ensemble-mean) AMO-like component of these residuals shows a pattern with some common features across 38 members as indicated by stippling) and multidecadal timescale; arguably, it represents the delayed forced response of individual models.

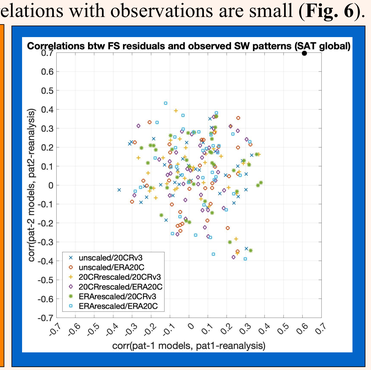

Fig. 6: Spatial correlations between AMO-like and AMO-orth patterns of individual forced-signal residuals and the corresponding patterns from either 20CRv3 or ERA-20C reanalysis. The black dot shows the correlations between the two reanalyses, which is well outside of the inter-model spread of correlations.

Discussion

Understanding the discrepancies between the observed and simulated multidecadal climate variability constitutes one of the pressing problems in climate science. These discrepancies manifest a coherent global signal which may reflect biases in the simulated response to external forcings or point to the observed internal variability unmatched by the climate models. This study provides a compact characterization of the global-scale forced responses in terms of just a few dominant patterns common across an ensemble of state-of-the-art climate models and the residual forced variability of individual models. The relative amplitudes of these patterns gauge climate sensitivity of individual models, while the residual signals have by far insufficient magnitude to explain the observed multidecadal climate undulations on top of the secular warming trend, and different spatial patterns. The results are documented in Kravtsov et al. (2024, 2025).

References

Deser, C. & Phillips, A. An overview of decadal-scale sea surface temperature variability in the observational record. *CLIVAR Exchanges* **72**/*PAGES Magazine* **25**, joint issue, 2–6 (2017). https://doi.org/10.22498/pages.25.1.2

Ghil, M. & Coauthors. Advanced spectral methods for climatic time series. *Rev. Geophys.* **40**, 1003 (2002). doi:10.1029/2000RG000092

Kravtsov, S., C. Grimm, and S. Gu, 2018: Global-scale multidecadal variability missing in the state-of-the-art climate models. *npj Climate and Atmospheric Science*, **1**, 34, doi:10.1038/s41612-018-0044-6, https://www.nature.com/articles/s41612-018-0044-6.

Kravtsov, S., A. Westgate, and A. Gavrilov, 2025: Global-scale multidecadal variability in climate models and observations. Part I: Forced response. *J. Climate*, **38**, 1829–1853, https://doi.org/10.1175/JCLI-D-24-0456.1.

Kravtsov, S., A. Westgate, and A. Gavrilov, 2024: Global-scale multidecadal variability in climate models and observations. Part II: The stadium wave. *Climate Dynamics*, **62**, 10281–10306. https://doi.org/10.1007/s00382-024-07451-4

Poli, P., H. Hersbach, D. Dee, and Coauthors, 2016: ERA-20C: An atmospheric reanalysis of the twentieth century. *J. Clim.* **29**, 4083–4097, doi:10.1175/JCLI-D-15-0556.1.

Slivinski, L. C., Compo, G. P., Whitaker, et al. 2019: Towards a more reliable historical reanalysis: Improvements for version 3 of the Twentieth Century Reanalysis system. Q. J. R. Meteorol. Soc., **145**; 2876–2908. doi:10.1002/qj.3598.and open access NOAA IR.

Wills, R. C. J., D. S. Battisti, K. C. Armour, T. Schneider, and C. Deser, 2020: Pattern Recognition Methods to Separate Forced Responses from Internal Variability in Climate Model Ensembles and Observations. *J. Climate*, **33**, 8693–8719, https://doi.org/10.1175/JCLI-D-19-0855.1.

Wills, R.C. J., Y. Dong, C. Proistosecu, K. C. Armour, and D. S. Battisti, 2022: Systematic climate model biases in the large-scale patterns of recent sea-surface temperature and sea-level pressure change. *Geophys. Res. Lett.*, **49**, e2022GL100011. https://doi.org/10.1029/2022GL100011.

Wyatt, M., S. Kravtsov, and A. A. Tsonis, 2012: Atlantic Multidecadal Oscillation and Northern Hemisphere's climate variability. *Clim. Dyn.*, **38**, 929–949, DOI 10.1007/s00382-011-1071-8.

Acknowledgments

We acknowledge the World Climate Research Programme's Working Group on Coupled Modelling, which is responsible for CMIP and thank the climate modelling groups for making their model output available. Support for the Twentieth Century Reanalysis Project data set is provided by the U.S. Department of Energy, Office of Science Innovative and Novel Computational Impact on Theory and Experiment (DOE INCITE) programme, and Office of Biological and Environmental Research (BER), and by the National Oceanic and Atmospheric Administration Climate Program Office. S. K. and A. W. were supported by the University of Wisconsin-Milwaukee's 2023 Finish Line grant.

For further information

Please contact *kravtsov@uwm.edu*. A PDF-version of this poster is available from https://sites.uwm.edu/kravtsov/presentations/